Journal of Integrative Agriculture 2026, 25(2): 694–708

Available online at ScienceDirect

Journal of Integrative Agriculture



RESEARCH ARTICLE

ScD27.2 gene regulation mechanism during sugarcane tillering and growth

Zhuandi Wu[1, 2], Xin Hu[1, 2], Wenzhi Wang[3], Zhengying Luo[1, 2], Naveed ur Rehman[1, 2], Peifang Zhao[1, 2], Jiayong Liu[1, 2], Shuzhen Zhang[3], Fenggang Zan[1, 2#], Xinlong Liu[1, 2#], Jiawen Guo[1, 2#]

[1] *National Key Laboratory for Biological Breeding of Tropical Crops of Ministry of Science and Technology, Kunming 650205, China*
[2] *Sugarcane Research Institute, Yunnan Academy of Agricultural Sciences/Yunnan Key Laboratory of Sugarcane Genetic Improvement, Kaiyuan 661699, China*
[3] *Institute of Tropical Bioscience and Biotechnology, Chinese Academy of Tropical Agricultural Sciences, Haikou 571101, China*

Highlights

- *ScD27.2* bidirectionally regulates sugarcane tillering: RNA interference of *ScD27.2* results in increased tillering whereas overexpression leads to reduced tillering, demonstrating the negative regulatory role of *ScD27.2* in tillering and establishing it as a potential target for plant architecture modification.
- Under drought stress, *ScD27*-RNAi lines exhibit a dwarf, multi-tillering phenotype, accompanied by a marked decrease in strigolactones (SLs) content and compromised yield. This indicates that *ScD27.2* modulates the balance between tillering and stress resistance by regulating SL biosynthesis.
- The presence of abiotic stress-responsive elements in the *ScD27.2* promoter, along with its regulation by the transcription factor *ScMYB44*, reveals part of the molecular network coordinating tillering and drought response.

Abstract

Tiller number represents a critical agronomic trait determining sugarcane yield. Strigolactones (SLs) are plant hormones regulating plant architecture. D27, an essential enzyme in the SL biosynthetic pathway, catalyzes a reversible isomerization reaction. *ScD27.2*, the *D27* homolog in sugarcane, contains abiotic stress-responsive elements in its promoter, suggesting its potential importance in SL biosynthesis and stress tolerance. *ScD27.2* potentially optimizes sugarcane agronomic traits, particularly tiller number and yield. Understanding its mechanisms will advance the development of high-yielding, stress-tolerant sugarcane varieties. To investigate the role of *D27* in sugarcane tillering, the key carotene isomerase gene *ScD27.2* was silenced (*via* RNAi) and overexpressed (OE) in sugarcane cultivar 'XTT22' plantlets. *ScD27*-RNAi-2 sugarcane exhibited decreased *ScD27.2* expression and increased tiller numbers compared to the wild type 'XTT22'. Conversely, overexpression lines (*ScD27*-OE-1, *ScD27*-OE-5, and *ScD27*-OE-9) showed increased *ScD27.2* expression and decreased tiller numbers. *ScD27*-OE-9 demonstrated notable lateral bud germination, while *ScD27*-RNAi-2 exhibited reduced drought tolerance. Under normal light and water management conditions, transgenic sugarcane plants showed significant differences in tiller number and plant height. During extended drought conditions, *ScD27*-RNAi-2 height was significantly reduced compared to wild type 'XTT22' and *ScD27*-OE-9, manifesting a dwarf, multi-tiller phenotype. Additionally, *ScD27*-RNAi-2 showed significantly reduced SLs content. These findings demonstrate that *ScD27.2* regulates tillering under drought stress, likely through SL biosynthesis, and that its drought response may be mediated by the transcription factor *ScMYB44*.

Keywords: DWARF27, carotene isomerase, drought stress response, strigolactone biosynthesis, tillering

Received 31 October 2024; Received in revised form 11 December 2024; Accepted 18 March 2025; Available online 18 April 2025
Zhuandi Wu, E-mail: judith1123@126.com; #Correspondence Fenggang Zan, E-mail: fengang88@126.com; Xinlong Liu, E-mail: lxlgood868@163.com; Jiawen Guo, E-mail: 79jwguo@163.com

© 2026 CAAS. Publishing services by Elsevier B.V. on behalf of KeAi Communications Co. Ltd. This is an open access article under the CC BY-NC-ND license (http://creativecommons.org/licenses/by-nc-nd/4.0/). Peer review under responsibility of Editorial Board of *Journal of Integrative Agriculture*.
doi: 10.1016/j.jia.2025.04.017

1. Introduction

Sugarcane (hybrids of *Saccharum* spp.) represents the predominant sugar-producing crop and a crucial bioenergy source, highlighting its importance in both agricultural and renewable energy sectors (de Abreu *et al.* 2020). Sugarcane demonstrates distinctive characteristics in yield composition compared to crops such as rice, flowers, and soybean. Specifically, sugarcane yield correlates strongly with sucrose content, stalk diameter, effective stalk count, and plant height, which directly influence its overall productivity (Lofton *et al.* 2012; Dias and Sentelhas 2018). The stalk constitutes the primary harvested component of sugarcane, with tiller quantity significantly determining crop yield. Thus, tiller number serves as an essential breeding index during varietal development (Kandel *et al.* 2018; Meena *et al.* 2022).

The tillering process in sugarcane encompasses three distinct phases: an initial phase of maximum tiller germination, the subsequent tiller growth cessation stage, and the tiller mortality stage preceding harvest. The tiller number maintains relative stability throughout this period until crop maturity and harvest, representing a critical aspect for yield optimization (Wang *et al.* 2023).

Multiple factors contribute to the eventual degenerative development of tillers, including inter-tiller competition, nutritional conditions, environmental factors, diseases, and insect pests. The initial maximum germinating tiller count correlates strongly with the millable stalk count at harvest. Significant variations exist in tiller rates among sugarcane varieties (Aitken *et al.* 2008). Our research demonstrated diverse tillering rates among sugarcane varieties, with '14NG124', 'KARA KARA WA', and 'XTT22' showing high rates exceeding 200%, while 'Badila', 'Cheribon', and 'Loether' exhibited substantially lower rates below 20%, adversely affecting their yield (Hemaprabha *et al.* 2022). Therefore, a high tillering rate remains essential for abundant millable sugarcane stalks (Wang *et al.* 2023).

Plant tillering undergoes regulation by specific plant hormones, with strigolactones (SLs) functioning to inhibit plant tillering, control overall plant morphological structures, and influence yield formation (Gomez-Roldan *et al.* 2008; Umehara *et al.* 2008). SLs comprise a category of carotenoid terpene lactone derivatives produced in plant roots that regulate drought resistance (Ha *et al.* 2014), cold tolerance (Cooper *et al.* 2018), salt tolerance (Mach 2015), stress (Stirnberg *et al.* 2012; Saeed *et al.* 2017), photomorphogenesis (Wei *et al.* 2016), and other growth and development traits in plants. SL biosynthesis results from carotenoid cleavage, involving several enzymes in the MAX/RMS/D pathway.

DWARF27(D27), a chloroplast-localized β-carotene isomerase, catalyzes reversible isomerization of all-*trans*-β-carotene to 9-*cis*-β-carotene, initiating the MAX/RMS/D pathway. Subsequently, CAROTENOID CLEAVAGE DIOXYGENASE 7 (CCD7) cleaves 9-*cis*-β-carotene to produce 9-*cis*-β-apo-10´-carotene (Arite *et al.* 2007; Lin *et al.* 2009; Alder *et al.* 2012; Al-Babili and Bouwmeester 2015).

After incorporating three oxygen molecules into 9-*cis*-β-apo-10´-carotenal, CCD8 initiates a molecular rearrangement process connecting carotenoids to SLs, ultimately producing a bioactive SL compound (Zhang *et al.* 2010; Iyer-Pascuzzi *et al.* 2011; Batra *et al.* 2019). The mechanism of isomerization catalyzed by D27 remains unclear, and D27 represents the only enzyme in SL biosynthesis requiring a metal cofactor (Al-Babili and Bouwmeester 2015).

The plant hormone abscisic acid (ABA) serves a vital role in plant response to drought stress (Hirayama and Shinozaki 2007). Increased ABA levels primarily arise from enhanced activity of the 9-*cis*-epoxide carotenoid dioxygenase (NCED) family, which catalyzes the rate-limiting step in ABA synthesis (Frey *et al.* 2012). Both SLs and ABA are involved in carotenoid cleavage and originate from a common carotenoid substrate (Liu *et al.* 2015). Thus, the connection between SL and ABA metabolism is inherent. The interaction between the SL and ABA pathways occurs through D27, which plays an essential role in mediating ABA and SL content communication in rice (De Smet *et al.* 2003; Wen *et al.* 2016; Yang *et al.* 2023). In a rice *d27* mutant incapable of producing SLs, tiller number increased while plant height decreased, and its phenotype was restored through exogenous SL application, demonstrating that D27 is essential for SL biosynthesis (Lin *et al.* 2009; Tolnai *et al.* 2024).

Previous studies have demonstrated that *D27* exhibits high expression in the shoot apical meristem and axillary bud and is induced by various treatments, including polyethylene glycol (PEG), salt stress, phosphate deficiency, and nutrient deficiency (Wu *et al.* 2017). In *Arabidopsis thaliana*, *DWARF27* encodes 9-*cis*/all-*trans*-β-carotene isomerase and responds to auxin, ABA, and phosphate deficiency (Abuauf *et al.* 2018). Under phosphate-deficient conditions, genes involved in SL biosynthesis, including those encoding D27, CCD7, CCD8, and rice MORE AXILLARY GROWTH 1 (OsMAX1), showed elevated expression in rice roots (Czarnecki *et al.* 2014; Bari *et al.* 2021), accompanied by increased SL content (Umehara *et al.* 2010). The expression levels of SL biosynthesis genes, specifically *MtCCD7*, *MtCCD8*, and *MtD27*, in *Medicago truncatula* roots were enhanced under phosphate deficiency (Brewer *et al.* 2013; Rasmussen *et al.* 2013; Ruyter-Spira *et al.* 2013). Research has shown that D27 responds to various treatments, with notably increased expression in both rice and *M. truncatula* under phosphate deficiency (Brewer *et al.* 2013; Rasmussen *et al.* 2013; Ruyter-Spira *et al.* 2013). The *DWARF27* (*D27*) gene in *A. thaliana* responds to auxin and ABA under phosphate deficiency (Rasmussen *et al.* 2013). Furthermore, elevated SL levels significantly enhance plant drought tolerance. Consequently, D27 may serve as a connecting element that synergistically increases ABA content, thereby enhancing plant drought tolerance (Liu *et al.* 2015; Cheng *et al.* 2017; Abuauf *et al.* 2018).

Light is detected by photoreceptors, including phytochromes and cryptochromes, which transform light signals into biochemical signals within plants (Koltai *et al.* 2011; Bharti *et al.* 2015). Specific treatments within the photosignal transduction pathway may indirectly affect *D27* gene expression levels (Wen *et al.* 2016). Currently, direct investigations into the relationship between the *D27*

gene and light remain limited. However, considering light's fundamental role as an essential condition for plant growth and development, it likely modulates plant branching and architecture through its influence on SL synthesis and *D27* gene function (Yuan *et al.* 2018). Analysis of *D27* gene expression levels under various light conditions may reveal direct effects of light on *D27* gene expression.

To investigate the function of sugarcane *D27*, analyses were conducted on its promoter sequence, subcellular localization, and *in situ* tissue-specific expression. Additionally, transgenic sugarcane lines with overexpression or silencing of *D27* were generated. The phenotypes and expression patterns under various stress conditions were examined to elucidate the biological functions of *D27*.

2. Materials and methods

2.1. Plant materials and growth conditions

Sugarcane cultivar 'XTT22' plantlets were established in the field at the Sugarcane Research Institute, Yunnan Academy of Agricultural Sciences in October 2018. Transgenic sugarcane seedlings (60-d-old) were initially transplanted into planting cups in a greenhouse before transfer to outdoor planting buckets.

2.2. Analysis of *ScD27.2*, its promoter sequence, and promoter activity

Smart search was utilized to identify the functional domain of the *ScD27.2* gene (GenBank accession: KP987221.1), and potential conserved domains in *ScD27.2* were analyzed. The *ScD27.2* sequence was examined within the sugarcane *Saccharum spontaneum* L. genome using BioEdit software. Homologous genes of *ScD27.2* in sugarcane were identified through genome comparison. The intron–exon structure of sugarcane *ScD27.2* was determined using the GSDS website (https://gsds.gao-lab.org/). The phylogenetic tree was constructed using the MEGA program (version 4.0) (http://www.megasoftware.net/mega.html).

The full-length DNA sequence of *ScD27.2* was isolated using a Genome Walking Kit (TaKaRa, Dalian, China). Genomic DNA was extracted from young leaves of sugarcane variety 'XTT22' using a Plant DNA Isolation Kit (TaKaRa). The primers are shown in Appendix A. For phylogenetic tree construction, amino acid sequences were aligned using Clustal W (http://www.clustal.org) from MEGA Version 5.0 (http://www.megasoftware.net/mega.html). The alignments were processed in MEGA version 5.0 for neighbor joining tree analysis. The sequences upstream and downstream of the coding sequence were amplified using a Genome Walking Kit (TaKaRa). The PCR fragment was cloned into a pMD19-T vector (TaKaRa) and sequenced. The upstream promoter sequences were analyzed using the Plantcare database (http://bioinformatics.psb.ugent.be/webtools/plantcare/html/).

The obtained target promoter was truncated into fragments of 1,700, 1,200, and 600 bp and subsequently ligated into the multicloning site of the pGreen II 0800-LUC plasmid, generating D27 Pro-1700, D27 Pro-1200, and D27 Pro-600 constructs, respectively, which were confirmed through sequencing. *Agrobacterium tumefaciens* strain EHA105 was employed to transform the constructs into 4-wk-old tobacco plants. Each plasmid was individually agroinfiltrated into two tobacco plants and incubated at 25°C for 14 h under continuous light. At 48 h post-injection, leaf segments measuring 0.5 cm×0.5 cm at the *Agrobacterium* injection site were collected for analysis. Luciferase activity was measured using a dual-luciferase detection kit (Promega, Madison, WI, USA; E1910) based on the fluorescence values recorded by the reporting system. The fluorescence value of the target gene plasmid divided by the reference plasmid (F/R value) was calculated. This value was compared to that of the control group, and the standard error was determined. The resulting data were used to generate a histogram.

2.3. *In situ* hybridization

RNA *in situ* hybridization was conducted to examine the distribution of *ScD27.2* mRNA in 45-d-old sugarcane plants. Roots, stalks, and buds of sugarcane lines underwent fixation, sectioning, and subsequent hybridization with probes (Pena *et al.* 2009; Sun *et al.* 2014). The probes were generated through PCR using gene-specific primers (Appendix A) that incorporated SP6 and T7 binding sites. The gene-specific primer sequences were as specified (Appendix A). Images were captured using an Olympus BX53 microscope (Olympus, Tokyo, Japan). The complete coding region of the *ScD27.2* gene was fused with Green Fluorescent Protein (GFP) in the pBWA(V)HS-Glosgfp vector to construct a 35S::ScD27-GFP expression vector and introduced into *A. thaliana* protoplasts. A co-expression marker plasmid served as the positive control.

2.4. Subcellular localization of GFP-tagged D27 in *A. thaliana* protoplasts

The PMD-18T-*ScD27* plasmid containing the *ScD27.2* gene fragment was digested with *Apa*I and *Spe*I enzymes. The resulting *ScD27.2* fragment was inserted into the pBWA(V) HS-Glosgfp vector. Expression of GFP-fused *ScD27.2* was controlled by the 35S promoter, yielding the pBWA(V)HS-*ScD27*-Glosgfp vector. *Arabidopsis thaliana* protoplasts were cultivated and isolated according to Yoo *et al.* (2007). The PEG-mediated method was utilized to transiently transform *A. thaliana* protoplasts with the 35S::ScD27-GFP construct (Zou *et al.* 2006). Subsequently, 0.2 mL of protoplast suspension in 20% PEG4000 (0.5×10^6 cells mL^{-1}) was combined with 20 μg of the Puc-GFP-*ScD27* plasmid and incubated at 23°C for 15 min in darkness. The transformed protoplasts were examined using a Zeiss Confocal Microscope (Zeiss, Oberkochen, Germany).

2.5. Construction of plant expression vectors

Construction of an RNA interference (RNAi) silencing expression vector A 400-base pair (bp) fragment of the *ScD27.2* gene was amplified from cDNA extracted from the apical meristem of sugarcane stalks. The primers, designed based on the multiple cloning site of the RNAi expression vector (pTCK303), are listed in Appendix A . Following double digestion with *Sac*I and *Spe*I enzymes as well as *Bam*HI and *Kpn*I enzymes, both forward and reverse orientations of the

targeted 400-bp fragment were isolated and ligated into the pTCK303 plasmid vector. This generated the expression vector pTCK303-*ScD27*-RNAi containing the positive and negative RNAi target regions. The PCAMBIA3301 plant expression vector was modified to include both forward and reverse *ScD27.2* fragments, each controlled by the 35S promoter, through double digestion using *Sma*I and *Hind*III restriction enzymes. This produced the plant RNAi silencing expression vector PCAMBIA3301-GUS-*ScD27*-RNAi, containing a *GUS* (encoding β-glucuronidase) reporter gene and an herbicide resistance gene (*bar*).

Construction of a *ScD27.2* overexpression vector Using the multiple cloning site (MCS) of the pCAMBIA3301 overexpression vector, primers were designed to amplify the full-length open reading frame (ORF) of the *ScD27.2* gene, with specific primers listed in Appendix A. The pCAMBIA3301 expression vector and amplified fragment underwent digestion with restriction enzymes *Nco*I and *Bgl*II. After digestion, the amplified fragment was inserted into the pCAMBIA3301 overexpression vector to construct the pCAMBIA3301-*ScD27*-overexpressed (OE) vector, controlled by the 35S promoter, for *ScD27.2* gene overexpression.

The constructed plant expression vector was transformed into *A. tumefacien*s strain EHA105, which was cultivated on YEP medium containing 10 g L^{-1} yeast extract, 10 g L^{-1} peptone, and 5 g L^{-1} NaCl, with antibiotics (50 mg L^{-1} kanamycin, 50 mg L^{-1} streptomycin, and 20 mg L^{-1} rifampicin).

2.6. *Agrobacterium*-mediated transformation of sugarcane plants

Under sterile conditions, the upper leaf sheaths of sugarcane 'XTT22' plants were removed. The immature whorled leaves were sectioned into 1-mm-thick rounds for embryogenic callus induction and preparation of immature sugarcane leaf cross-sections (Bohorova *et al.* 1999). Transverse sections of approximately 1 mm thickness were obtained directly from the meristem and placed on callus induction medium comprising MS medium supplemented with 30 g L^{-1} sucrose, 2 mg L^{-1} 2,4-D (2,4-dichlorophenoxyacetic acid), and 8 mg L^{-1} agar (Murashige and Skoog 1962). These were maintained at 28°C in darkness, with medium replacement every 2 wk. After 45 d, light yellow and firm calli were selected and finely divided prior to transformation.

The *in vitro A. tumefacien*s culture was centrifuged and resuspended in infection medium (1/5 strength MS medium C, 30 g L^{-1} sucrose, 30 g L^{-1} glucose, 100 mmol L^{-1} acetosyringone), then diluted to an OD_{600} of 0.5–1.0. The callus was immersed in the *Agrobacterium* infection solution containing expression vectors and gently agitated in darkness for approximately 30 min. After removing the *Agrobacterium* suspension, the callus was transferred to a Petri dish, and excess suspension was removed using filter paper. Following 30 min of air-drying in a sterile environment, the callus was transferred to fresh medium containing 2 mg L^{-1} of 2,4-D and incubated at 22°C in darkness for 7 d.

The transformed callus was transferred to screening medium (MS, 2.0 mg L^{-1} 2,4-D, 8 g L^{-1} agar, 200 mg L^{-1} Timentin, 5 g sucrose, 0.05% Basta) and maintained for 35 d at 28°C in darkness. Resistant calli were transferred to regeneration medium (MS, 1.0 mg L^{-1} 6-BA (6-Benzylaminopurine), 8 g L^{-1} agar, 200 mg L^{-1} Timentin, 5 g sucrose, 0.05% Basta) and cultured under light for 14 d. Emergent green shoots were transferred to rooting medium (MS, 2 mg L^{-1} NAA (1-Naphthaleneacetic acid), 8 g L^{-1} agar, 300 mg L^{-1} Timentin, 5 g sucrose, 0.05% Basta) and maintained under light at 28°C for 20 d. Individual shoots were subsequently transferred to fresh rooting medium for an additional 20 d. Leaves from resistant seedlings were collected for molecular analysis before soil transplantation.

2.7. PCR detection

Genomic DNA from sugarcane leaves was extracted using a Plant DNA Isolation Reagent Kit (TaKaRa). The target fragments of the *ScD27.2* gene and the *bar* gene were detected using PCR (primers listed in Appendix A). PCR products were analyzed using 1.0% agarose gel electrophoresis.

2.8. Detection of *GUS* expression

GUS expression analysis followed methods described by Cao *et al.* (1998) and Zhou *et al.* (2001). Histochemical staining was performed on freshly dissected sugarcane leaves to evaluate *GUS* activity. A Zeiss AxioScope 2 Plus microscope was used to capture images.

2.9. Phenotype evaluation

Phenotypic observation was conducted at maturity (180 d) to identify stable and significantly different lines. Overexpression lines (*ScD27*-OE-9, *ScD27*-OE-5 and *ScD27*-OE-1) and RNAi lines (*ScD27*-RNAi-2 and *ScD27*-RNAi-6) were selected for further tillering phenotype assessment. Height, diameter, Brix and stalk number measurements were taken from the silenced and OE lines of sugarcane seedlings. Stalk number, sugarcane yield, actual weight, and theoretical sugar yield were evaluated. Sugar content and sucrose yield calculations used the following formulae: Sucrose content (%)=Brix×1.0825−7.703; Sucrose yield (t ha^{-1})=Cane yield (t ha^{-1})×Sucrose content (%).

2.10. Expression of the sugarcane *ScD27.2* gene

Total RNA was extracted from 45-d-old 'XTT22' sugarcane tissue using Trizol (Invitrogen, Waltham, MA, USA) for quantitative real-time reverse transcription PCR (qRT-PCR). RNA quality assessment utilized 1% agarose gel electrophoresis, with spectrophotometric quantification (DR3900). First-strand cDNA synthesis employed a Reverse Transcriptase M-MLV (RNase H^-) Kit (TaKaRa). qRT-PCR was performed using a Prime Script RT Reagent Kit with gDNA Eraser and SYBR Premix *Ex Taq* II Kit (TaKaRa) in a 20 μL reaction. Primers are listed in Appendix A. The *ScD27.2* gene expression was analyzed using the ABI Vii7 real-time PCR System (Applied Biosystems, Foster City, CA, USA). Fluorescence quantitative analysis utilized the SYBR Green Kit (TaKaRa), following manufacturer's protocols.

Relative gene expression levels were calculated using

the comparative cycle threshold (CT) method (Livak and Schmittgen 2001). *GAPDH* (encoding glyceraldehyde-3-phosphate dehydrogenase) served as an internal reference gene, with primers shown in Appendix A . Non-transformed 'XTT22' sugarcane served as the negative control. Each sample underwent three technical replicates, with three biological replicates per treatment to ensure data reproducibility and statistical significance.

2.11. Dark treatment

Silenced and OE lines of sugarcane seedlings were cultivated under sterile conditions until 5–6 new leaves emerged. Before dark treatment, seedlings were maintained under a normal light/dark cycle (16 h light/8 h dark) at 28°C for 4 wk with artificial light intensity of 100–120 μmol m^{-2} s^{-1}. Subsequently, seedlings were exposed to continuous darkness. The experiment commenced upon dark transfer, with sampling at 0, 1, 6, 12, 24, and 36 h. The upper shoot apical meristem was harvested after removing leaves and leaf sheaths. Samples were flash-frozen in liquid nitrogen and stored at −80°C. Each treatment included 3 replicates, with 10–12 plants per replicate.

2.12. Hydroponic culture

The silenced and OE lines of sugarcane seedlings were cultivated under sterile conditions for 3 wk until reaching 8–10 cm in height. At 3 d after opening the plant-containing bottle, the medium was removed from the roots, and the plants were transferred to hydroponic solution containing 0.65 mmol L^{-1} $MgSO_4$, 2 mmol L^{-1} NH_4NO_3, 2 mmol L^{-1} CaCl2, 0.75 mmol L^{-1} K_2SO_4, 0.1 mmol L^{-1} KCl, 0.25 mmol L^{-1} KH_2PO_4, 0.2 mmol L^{-1} Fe-EDTA, 1×10^{-3} mmol L^{-1} $MnSO_4$, 1×10^{-3} mmol L^{-1} $ZnSO_4$, 1×10^{-4} mmol L^{-1} $CuSO_4$, 5×10^{-6} mmol L^{-1} $(NH_4)_6Mo_7O_{24}$, and 1×10^{-3} mmol L^{-1} H_3BO_3. The pH was adjusted to 6.0 using 3 mol L^{-1} KOH. For the low P solution, KH_2PO_4 was substituted with 0.3475 mmol L^{-1} KCl. Seedlings were maintained in an incubator at 25/20°C with a 16/8 h light/dark photoperiod and light intensity of 100–120 μmol m^{-2} s^{-1}. The seedlings underwent hydroponic cultivation for 12 d before phosphate deficiency treatment. At 0, 6, 12, 24, and 48 h after treatment, the upper portion of the leaves (excluding buds and stalks) was collected. Each sample had 3 replicates, with 10–12 plants per replicate. The samples were flash-frozen in liquid nitrogen and stored at −80°C.

2.13. Drought tolerance and water loss assays

The silenced and OE lines of sugarcane seedling stalks were grown in 1-L pots to examine drought stress effects on sugarcane. The selected stalks were uniform in size, and the river sand quantity was standardized across all pots. During the experiment, water was administered uniformly to minimize experimental variation. Initially, the plants were fully irrigated until reaching 4 wk of age. The treatments comprised: short-term drought treatment (15 d), extended drought stress treatment (120 d), drought stress survival assessment, and water deficiency rate measurement.

For short-term drought treatment, 4-wk-old silenced and OE lines of sugarcane seedlings were maintained at 45% of field capacity (FC) for 15 d. Shoot apical meristems were harvested at 10:00 am on d 0, 1, 4, 7, and 9. Each sample was replicated three times, utilizing three plants per replicate. The samples were immediately frozen in liquid nitrogen and stored at −80°C.

To evaluate drought effects on transgenic sugarcane, the plants underwent a long-term outdoor (open air) water control treatment for 120 d. The experiment included six repetitions, with 1 bud per pot, maintaining field water capacity at 30–50%.

Drought tolerance was evaluated through a survival test. Four-week-old sugarcane seedlings underwent drought treatment by withholding water for 12 d, followed by a 3-day recovery period with resumed irrigation. The survival rate was then calculated, with each sample replicated five times.

For water deficiency assessment, approximately 5 g of leaves were collected from 4-wk-old sugarcane plants. The leaves were weighed at predetermined intervals while maintained in identical conditions. Water loss was calculated relative to the initial leaf weight, and the water loss percentage was determined. This experiment included three replicates.

2.14. SL content determination in sugarcane root tissue

Following the methodology described by Haider *et al.* (2018), the SL content from harvested sugarcane roots underwent extraction and assessment with minor modifications. Fresh root tissue (0.8 g) was collected and pulverized into powder using liquid nitrogen. The pulverized sample was transferred to a 10 mL chilled glass tube, followed by addition of 2 mL ethyl acetate containing GR24 (with an internal standard (IS) of 0.01 nmol mL^{-1} ethyl acetate GR24 solution). Following ultrasonic grinding for 15 min, the samples underwent centrifugation at 1,000×g for 10 min. The organic phase was re-extracted with 2 mL of ethyl acetate and the extracts combined. The collected samples were dried using a vacuum dryer (Thermo Scientific SPD121P SpeedVac).

The residue underwent reconstitution in 50 mL of ethyl acetate and dilution with 4 mL of 100% hexane before application to a pre-assembled HBL 3 cc (60 mg) extraction cartridge (Oasis at Waters, Milford, MA, USA). After washing the cartridge with 2 mL of 100% hexane, SLs were eluted using a solvent mixture comprising 2 mL of hexane and ethyl acetate in a ratio of 10:90. Data acquisition and analysis utilized MassLynx 4.1 (TargetLynx) software (Waters). The concentrations of SLs, namely (±)-2'-epi-5-deoxystrigol and (±)-5-deoxystrigol, were quantified based on standard calibration curves and normalized using the IS. All experiments were conducted in triplicate, with results expressed as mean±standard deviation (SD).

2.15. Yeast one-hybrid (Y1H) assay

To investigate whether *ScMYB44* binds to the promoter fragments of *ScD27.2*, the study employed the Matchmaker Gold Yeast One-Hybrid Library Screening System (Clontech, TaKaRa, Shiga, Japan). The 1,561 bp promoter fragment of the *ScD27* gene was inserted into the pABAi vector.

The *ScMYB44* coding sequence (encoding a transcription factor) was incorporated into pGADT7. Background AbAr expression testing of the Y1HGold pAbAi-proSsD27 strain followed the user manual protocol. Subsequently, the interaction between the *ScMYB44* transcription factor and the promoter fragments of the *ScD27.2* genes underwent examination. The primers utilized in this assay are listed in Appendix A.

2.16. Statistical analysis

All experiments underwent three repetitions. Data represent the mean±standard error from a single experiment. Analysis of variance (ANOVA) was performed, followed by Duncan's test. Different letters denote significant differences (P<0.05) between different treatments.

3. Results

3.1. Analysis of the *ScD27.2* gene and promoter in the sugarcane genome

The functional domains of the *ScD27.2* gene underwent analysis using Smart search, revealing a conserved Domain of Unknown Function (DUF), DUF4033, in *ScD27.2*. Analysis of the *ScD27.2* sequence against the sugarcane *S. spontaneum* L. genome using BioEdit software (Altschul *et al.* 1997) indicated that *ScD27.2* represented a homologous gene of Sspon.06G0016140-2C.

Utilizing the RNA sequence of the *ScD27.2* gene as a template, primers were designed to isolate the complete genome sequence of the *ScD27.2* gene in sugarcane from DNA using the chromosome walking method. The intron–exon structure analysis of sugarcane *ScD27.2* through the GSDS website revealed seven exons and six introns (Fig. 1-A). Phylogenetic analysis of *ScD27.2* demonstrated that among 19 species, *ScD27.2* in 'XTT22' showed closest relation to maize *ZmD27* (Fig. 1-A). The gene structure analysis revealed that *ScD27.2* possesses a conserved genomic organization, characterized by the presence of seven exons and six introns. This architectural pattern is highly similar to that of its close orthologs in maize (*ZmD27*) and sorghum (*SbD27*), reinforcing the phylogenetic proximity and suggesting that the splicing pattern and potential regulatory elements within the introns may have been functionally conserved during evolution (Fig.1-B).

The chromosome walking method yielded the 1,762-bp sequence of *ScD27.2* located upstream of the open reading frame. Analysis of the *ScD27.2* promoter using the PlantCare

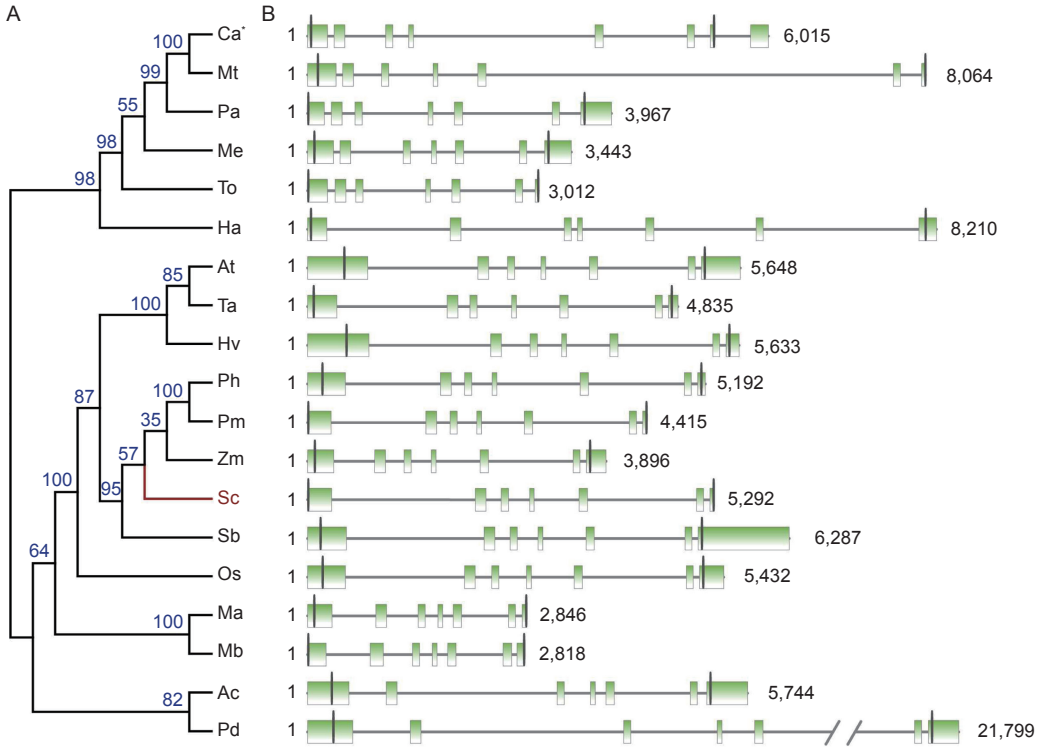


Fig. 1 Molecular phylogenetic tree and gene structure analysis of the *ScD27.2* gene in sugarcane (*Saccharum* hybrid cultivar 'XTT22'). A, molecular phylogenetic tree of D27 proteins from various plant species. The multiple sequence alignment was performed using MAFFT version 4. A neighbor-joining phylogenetic tree was constructed using MEGA 6 with 1,000 bootstrap replicates. Bootstrap values are shown at the nodes. The scale bar indicates the number of amino acid substitutions per site. Species abbreviations and GenBank/NCBI accession numbers are as follows: ScD27.2 (*Saccharum hybrid*, ALB35091), SbD27 (*Sorghum bicolor*, XP_021316884), PmD27 (*Panicum miliaceum*, RLM58430), PhD27 (*Panicum hallii*, XP_025828166), ZmD27 (*Zea mays*, NP_001144840), OsD27 (*Oryza sativa*, XP_015615253), HvD27 (*Hordeum vulgare*, BAJ90178), TaD27 (*Triticum aestivum*, KAF7103320), AetD27 (*Aegilops tauschii*, XP_020183166), MaD27 (*Musa acuminata*, XP_009402431), PdD27 (*Phoenix dactylifera*, XP_026663993), AcD27 (*Ananas comosus*, XP_020101063), MbD27 (*Musa balbisiana*, THU44729), MeD27 (*Manihot esculenta*, XP_021612504), PaD27 (*Prosopis alba*, XP_028758424), MtD27 (*Medicago truncatula*, RAH296), CaD27 (*Cicer arietinum*, XP_004495151), ToD27 (*Trema orientale*, PON94996), HaD27 (*Helianthus annuus*, XP_022005076). B, gene structure of ScD27.2. Exons are represented by yellow boxes, introns by black lines. The untranslated regions (UTRs) are shown as blue boxes. The scale at the bottom indicates the genomic length.

database revealed fundamental regulatory elements characteristic of eukaryotic promoters, including a TATA-box and CAAT-box. Further examination of the regulatory elements within the promoter region identified stress-responsive functional elements, including an ABA response element (ABRE), an anaerobic induction element (ARE), light response elements (I-box, G-box, BOX 4, GT1-Motif, TCCC-motif, TCT-motif), Methyl jasmonate response elements (CGTCA-Motif, TGACG-motif), a low-temperature response element (LTR), and a drought-induced MYB transcription regulatory factor binding site (MBS) (Appendix A).

The double luciferase assay demonstrated strong promoter activity in the full-length promoter. When truncated to 1,200 bp, the promoter activity remained unchanged; however, truncation to 600 bp resulted in a reduction of promoter activity by more than threefold. This observation indicates the presence of *cis*-acting elements affecting promoter activity within the 600–1,200 bp region (Fig. 2-A).

3.2. Localization and spatial distribution of *ScD27.2*

To further elucidate the function of *ScD27.2*, its subcellular localization was determined. Colocalization analysis utilized chlorophyll autofluorescence. Confocal laser microscopy analysis revealed red fluorescence in the plastid (Fig. 2-B), while the green fluorescence of GFP completely overlapped with the red fluorescence (chlorophyll autofluorescence). *ScD27.2* was localized in the plastid in *A. thaliana*. *ScD27.2* exhibited high expression in the vascular bundle of roots, stalks, and leaves (Fig. 3).

3.3. Detection and tillering phenotypes of transgenic sugarcane lines

PCR analysis confirmed that 8 RNAi lines and 12 overexpression lines were positive for the *bar* gene (Appendix B-a). Among the 12 overexpression transgenic lines, 11 showed PCR-positive results for *ScD27.2* (Appendix B-b). The PCR detection results confirmed the generation of 11 sugarcane lines overexpressing *ScD27.2* and 8 *ScD27*-RNAi lines (Table 1). All eight *SCD27*-RNAi sugarcane lines demonstrated positive β-GUS activity. The *GUS* staining results for *ScD27*-RNAi-2 are presented in Appendix C.

At maturity (180 d), tillering phenotypes were assessed in the overexpression (*ScD27*-OE-9, *ScD27*-OE-5, and *ScD27*-OE-1) and RNAi lines (*ScD27*-RNAi-2 and *ScD27*-RNAi-6) (Table 2). Significant differences in tiller number were observed between the transgenic lines and the wild type ('XTT22'). The wild type averaged 3.83 tillers, while RNAi lines exhibited significantly more tillers (8.00 in *ScD27*-RNAi-2 and 10.50 in *ScD27*-RNAi-6). The overexpression lines produced significantly fewer tillers than the wild type (1.50 in *ScD27*-OE-9, 2.33 in *ScD27*-OE-5, and 2.17 in *ScD27*-OE-1). Plant height showed no significant differences between overexpression lines and wild type; however, *ScD27*-RNAi-2 and *ScD27*-RNAi-6 were significantly shorter than both overexpression lines and wild type. Pot experiments demonstrated that RNAi lines *ScD27*-RNAi-2 and *ScD27*-RNAi-6 achieved significantly higher cane yields than wild type and overexpression lines, reaching 59.73 and 68.85 kg, respectively. The overexpression lines (*ScD27*-OE-9, *ScD27*-OE-5, and *ScD27*-OE-1) produced significantly lower cane yields than the wild type. No significant differences in Brix were observed between transgenic sugarcane and wild type (Table 2). The theoretical sucrose yield analysis aligned with the actual yield results (Table 2). *ScD27*-OE-9 displayed increased axillary bud sprouts (indicated by the black arrow in Fig. 4).

3.4. *ScD27.2* expression in transgenic lines

Overexpression (*ScD27*-OE-9, *ScD27*-OE-5, and *ScD27*-OE-1) and RNAi lines (*ScD27*-RNAi-2 and *ScD27*-RNAi-6) exhibiting stable and significant phenotypic differences compared with the wild type were selected for subsequent analysis (Fig. 5).

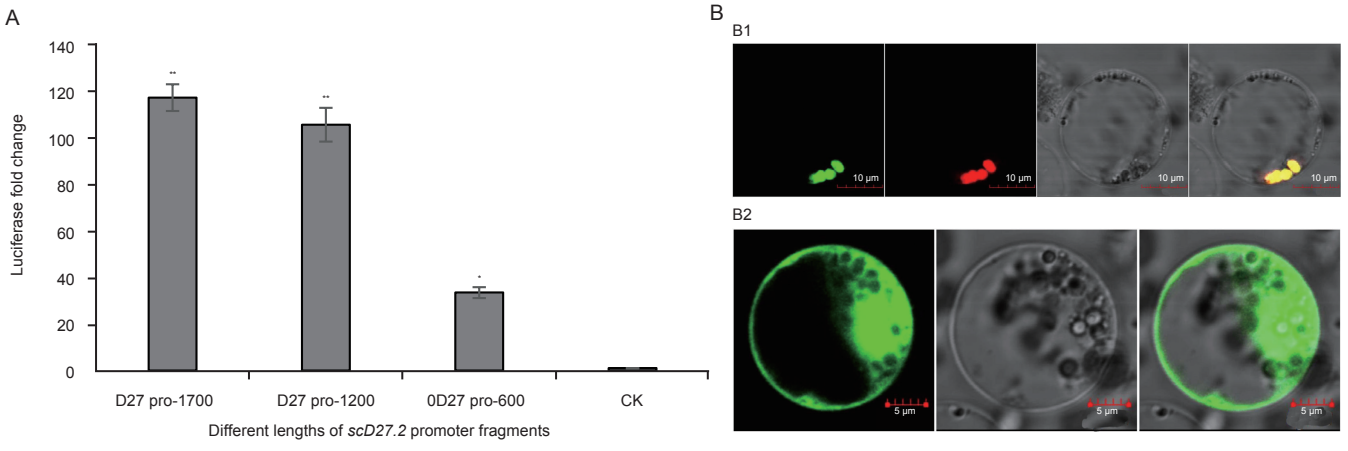


Fig. 2 Promoter activity, subcellular localization of *ScD27.2*. A, progressive 3′ deletion analysis of the sugarcane *ScD27.2* promoter. The relative luciferase activities of the pGreenII 0800-Luc plasmid containing D27Pro-1700, D27Pro-1200, and D27Pro-600 under lipopolysaccharide (LPS) stimulation are presented. Values represent mean±SD (n=3). *, significant at P<0.05; **, significant at P<0.01; Student's t-test. B, Subcellular localization of the ScD27.2 protein. B1, subcellular localization of the ScD27.2 protein; panels show target protein fluorescence channel, marker fluorescence channel, bright field, and merged image from left to right. B2, subcellular localization of control vectors without target genes; empty vector control showing fluorescence channel, bright field, and merged image from left to right.

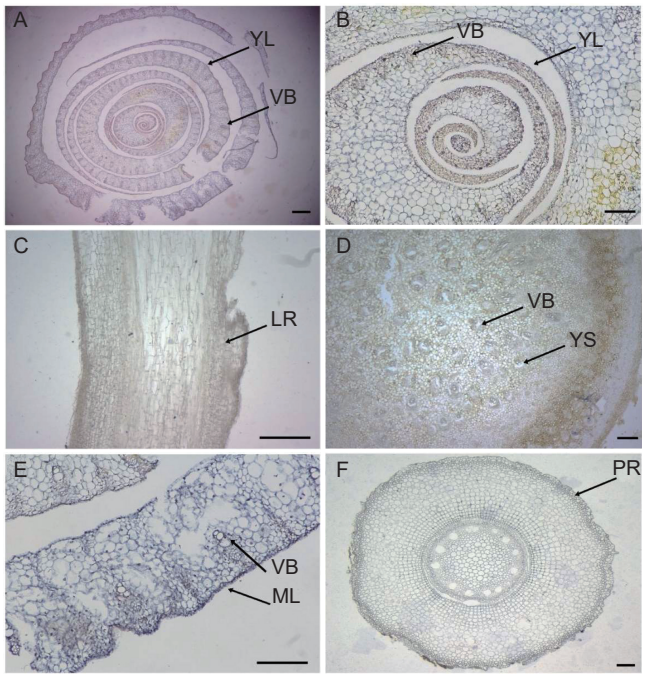


Fig. 3 Histochemical localization of *ScD27.2* using *in situ* hybridization in 45-d-old sugarcane seedlings. Expression of *ScD27.2* in young leaves (YL) (A and B); lateral roots (LR) (C); young stalk (YS) and vascular bundle (VB) (D); mature leaves (ML) and VB (E); primary root (PR) (F). Scale bars: (A) 50 μm; (B, E) 5 μm; (C, D, F) 20 μm.

The expression level of the *ScD27.2* gene in the shoot apical meristem of transgenic sugarcane was analyzed using qRT-PCR. The relative *ScD27.2* expression level in the shoot apical meristem of wild type 'XTT22' was normalized to 1, with a tiller number of 3.83. The relative *ScD27.2* expression levels were 4.14, 6.74, and 5.91, corresponding to tiller numbers of 1.5, 2.33, and 2.17 in *ScD27*-OE-9, *ScD27*-OE-5, and *ScD27*-OE-1, respectively. The relative expression levels were 0.52 and 0.33, with tiller numbers of 8.00 and 10.50 in *ScD27*-RNAi-2 and *ScD27*-RNAi-6, respectively. These results validated the upregulation and downregulation of *ScD27.2* expression in the overexpression and RNAi lines, respectively, demonstrating that the relative expression level of *ScD27.2* was negatively correlated with tiller number in transgenic lines (Fig. 5).

To assess whether *ScD27.2* was responsive to light,

Table 1 PCR analysis results for resistant shoots[1)]

Resistant shoots	*ScD27*-OE	*bar*	Resistant shoots	*ScD27*-OE	*bar*
OE-1	+	+	OE-11	+	+
OE-2	+	+	OE-12	+	+
OE-3	+	+	RNAi-1		+
OE-4	+	+	RNAi-2		+
OE-5	+	+	RNAi-3		+
OE-6	+	+	RNAi-4		+
OE-7	–	+	RNAi-5		+
OE-8	+	+	RNAi-6		+
OE-9	+	+	RNAi-7		+
OE-10	+	+	RNAi-8		+

[1)] "+" indicates positive PCR analysis results; "–" indicates negative PCR analysis results. PCR analysis identified eleven sugarcane lines overexpressing *ScD27.2* and eight *ScD27*-RNAi lines.

transcription of *ScD27.2* in the apical meristem of *ScD27*-OE-9, *ScD27*-RNAi-2, and 'XTT22' was measured under dark treatment for 0–36 h. As illustrated in Fig. 6-A, under dark treatment, the expression of *ScD27.2* was significantly downregulated in the buds of 'XTT22'. *ScD27.2* expression in *ScD27*-OE-9 exhibited a similar but more pronounced response to dark treatment compared to 'XTT22', while *ScD27*-RNAi-2 showed no significant change. These findings indicate that *ScD27.2* expression in seedlings is enhanced under light conditions and suppressed under dark conditions, confirming that the promoter sequence of the *ScD27.2* gene contained multiple photoactive elements (Appendix D).

To investigate whether *ScD27.2* responded to phosphate deficiency, the expression of *ScD27.2* was evaluated in phosphate-free hydroponic solution. *ScD27.2* expression was significantly upregulated in 'XTT22' under phosphate deficiency, particularly within 12 h. *ScD27*-OE-9 demonstrated a more rapid response to phosphate deficiency than 'XTT22'. In *ScD27*-OE-9, *ScD27.2* expression remained stable up to 6 h but increased after 12 h and rose rapidly at 24–48 h. However, in *ScD27*-RNAi-2, *ScD27.2* expression maintained a consistently low level and showed no significant change in response to phosphate deficiency (Fig. 6-B). *ScD27.2* expression was induced by phosphate deficiency, and the response correlated with the transcription level of *ScD27.2*.

3.5. *ScD27*-RNAi plants exhibited more tillering and dwarf phenotypes under drought conditions

To examine whether *ScD27.2* responded to drought stress,

Table 2 Agronomic characteristics and industrial traits in transgenic lines and the control lines at the mature stage (180 d)

Tr lines	Height (cm)	Diameter (cm)	Brix (%)	Stalk number[1)]	Cane yield (kg/6 barrels)	Theoretical sucrose yield (TSY) (kg/6 barrels)[2)]
OE-1	320.17±21.84 b	2.67±0.15 a	20.82±0.68 a	2.17±0.37 a	19.01±2.03 a	2.83±0.38 a
OE-5	341.33±14.02 b	2.60±0.14 a	20.95±1.02 a	2.33±0.47 a	24.58±3.21 ab	3.67±0.46 b
OE-9	329.17±16.44 b	2.73±0.15 a	20.72±0.41 a	1.50±0.50 a	23.12±4.02 b	3.40±0.56 b
RNAi-2	291.67±21.92 a	2.62±0.17 a	20.89±0.40 a	8.00±0.58 c	59.73±4.13 d	8.90±0.64 d
RNAi-6	281.67±15.72 a	2.55±0.13 a	20.68±0.28 a	10.50±1.50 d	68.85±9.49 d	10.09±1.33 d
CK	347.00±10.44 b	2.65±0.10 a	21.27±0.53 a	3.83±0.90 b	48.53±10.38 c	7.43±1.54 c

[1)] Stalk number is the total count per set of 6 barrels.
[2)] Theoretical sucrose yield (TSY) was calculated per 6 barrels using the formulas: Sucrose content (%)= Brix×1.0825−7.703; TSY (kg)=Cane yield (kg)×Sucrose content (%)/100.
Data are presented as mean±SD (n=3). Values within a column followed by different lowercase letters are significantly different at P<0.05 according to LSD test.



Fig. 4 Phenotypes of *ScD27*-RNAi-2 and *ScD27*-OE-9. A, comparison of wild type sugarcane ('XTT22'), *ScD27.2* gene overexpression line *ScD27*-OE-9, and RNAi-*ScD27* line *ScD27*-RNAi-2 under normal field conditions after 180 d of cultivation. B, non-transgenic sugarcane ('XTT22'). C, *ScD27.2* gene overexpression line *ScD27*-OE-9. D, RNAi-*ScD27* line *ScD27*-RNAi-2. *ScD27*-OE-9 exhibits increased axillary bud sprouting (indicated by black arrows).

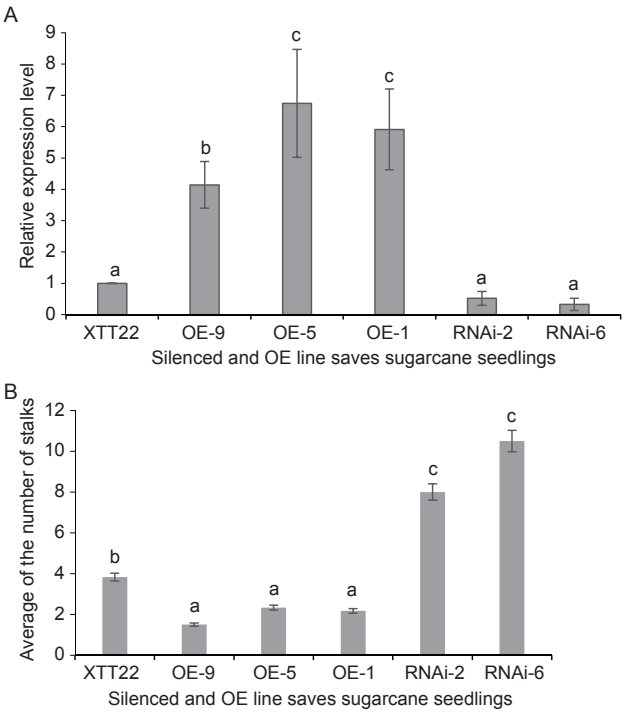


Fig. 5 *ScD27.2* expression and mean tillering in RNA interference lines (RNAi), *ScD27.2*-overexpressing transgenic lines (OE) and wild-type ('XTT22'). A, qRT-PCR analysis of *ScD27.2* transcription levels in each strain. *GAPDH* (encoding glyceraldehyde-3-phosphate dehydrogenase) transcription served as a cDNA normalization control. Data represent means of three biological replicates±SE; different letters above bars indicate significant differences (P<0.05) by Duncan's test. B, mean tillering number represents the average stalk count of sugarcane plants exceeding 0.5 m in height, shown as mean±SD (n=4).

ScD27.2 expression was evaluated under 45% field water capacity for 9 d. *ScD27.2* expression increased significantly in the wild type 'XTT22' control group under drought stress for up to 7 d (Fig. 6-C). In *ScD27*-OE-9 plants, *ScD27.2* expression remained stable within 4 d but increased significantly at d 7. *ScD27.2* expression in *ScD27*-RNAi-2 plants maintained a consistently low level and showed no significant change in response to drought stress. These results demonstrate that *ScD27.2* expression was induced by drought, and the drought stress response correlated with the transcription level of *ScD27.2*.

Under long-term outdoor drought stress (120 d), compared with the wild type, *ScD27*-RNAi-2 plants exhibited a dwarf phenotype, with a significantly increased number of tillers (9.60 on average) and a reduced plant height of 0.32 m. The phenotypes of *ScD27*-OE-9 and 'XTT22' remained similar under drought stress; the average number of tillers was 1.33 and 1.26, respectively, and the plant heights were 0.89 and 0.92 m, respectively (Fig. 7).

To investigate the contribution of *ScD27.2* to drought tolerance, we assessed the survival rate of *ScD27*-OE-9

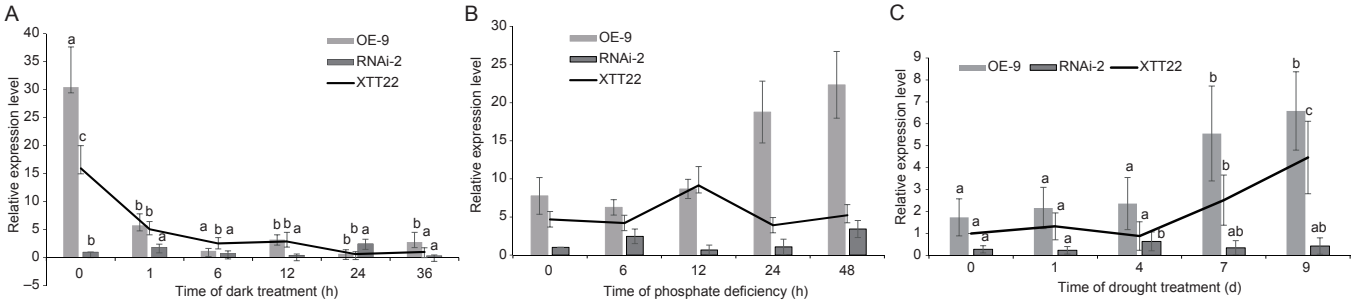


Fig. 6 Expression patterns of *ScD27.2* under dark (A), phosphate-deficient (B), and drought stress (C) conditions. In Fig. B, seedlings were transferred to a P-deficient solution and then sampled after 12 d of growth in a hydroponic solution with 1.0 mmol L^{-1} P; In Fig. C, drought stress was set at 45% field water capacity, with samples harvested from the shoot apical meristem. For all panels (A–C), expression levels were analyzed by qRT-PCR, with GAPDH as the internal reference gene for normalization. Data are presented as mean±SE of three biological replicates. Different lowercase letters above the bars within each time point indicate significant differences (P<0.05) among genotypes as determined by Duncan's test.



Fig. 7 Phenotypic characteristics of *ScD27*-RNAi-2, *ScD27*-OE-9, and 'XTT22' under extended outdoor drought stress (120 d). A and B, from left to right, *ScD27*-RNAi-2, *ScD27*-OE-9, and 'XTT22' plants following 120 d of open cultivation under prolonged drought treatment. Phenotypic responses of *ScD27*-RNAi-2 and *ScD27*-OE-9 under extended drought stress. C, phenotypic comparison of *ScD27*-RNAi-2 and *ScD27*-OE-9.

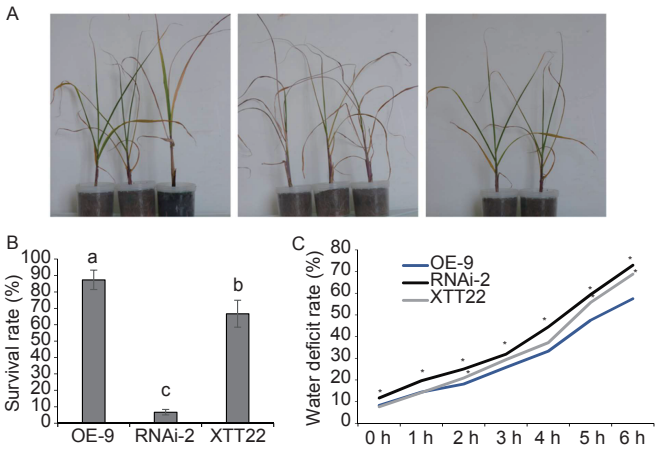


Fig. 8 Drought tolerance assessment of sugarcane *ScD27* transgenic lines. A, representative phenotypes of *ScD27*-OE-9, *ScD27*-RNAi-2, and wild type 'XTT22' plants subjected to 12-d drought stress followed by 3-d rehydration. The post-recovery survival rate is indicated (n=3). B, population survival rate after rehydration. Survival percentages were quantified on a larger scale (n=16). Data are mean±SE. Different lowercase letters indicate significant differences (P<0.05) by Duncan's multiple range test. C, leaf water deficit in mature plants. Water deficit rate was measured in mature leaves under drought conditions (n=9). Data are mean±SE. Significant differences compared to the wild type were determined by Student's t-test (*, P<0.05; **, P<0.01).

and *ScD27*-RNAi-2 under drought treatments. Compared with wild type 'XTT22', the survival rate of *ScD27*-OE-9 was 87.33%, which was 21% higher than that of the RNAi strain *ScD27*-RNAi-2, which demonstrated significantly reduced survival at only 12.6% (Figs. 8-A and B).

Transpiration loss represents one of the most critical parameters affecting drought sensitivity. Therefore, we measured the water deficiency rate in sugarcane leaves. The water deficiency rate in *ScD27*-RNAi-2 leaves was significantly higher than that in wild type and *ScD27*-OE-9 leaves (Fig. 8-C), and the water deficiency rate of *ScD27*-OE-9 was 11% lower than that of the wild type on d 6.

3.6. Reduced SL levels in the *ScD27*-RNAi lines

In the present study, two kinds of SLs, i.e., (±)-2′-epi-5-deoxystrigol and (±)-5-deoxystrigol, were detected under drought stress. Four-week-old *ScD27*-OE-9, *ScD27*-RNAi-2, and wild type 'XTT22' plants were used as test materials and maintained under 45% drought stress for 15 d. The SL content was measured in the root tissues. Under drought stress, the (±)-2′-epi-5-deoxystrigol content in *ScD27*-OE-9, *ScD27*-RNAi-2, and 'XTT22' plants reached 218.28, 25.63, and 184.31 ng g^{-1} of dry weight (DW), respectively. The (±)-5-deoxystrigol contents were 84.69, 20.90, and 81.29 ng g^{-1} DW, respectively. The analysis revealed that the contents of (±)-2′-epi-5-deoxystrigol and (±)-5-deoxystrigol were significantly reduced in *ScD27*-RNAi-2 plants compared to the wild type controls (Fig. 9).

3.7. The *ScMYB44* transcription factor interacts with the *ScD27.2* promoter

MYB44 transcription factors have been demonstrated to interact with the promoters of abiotic stress-responsive genes (Persak and Pitzschke 2014; Li *et al.* 2021; Wang *et al.* 2021). Based on the bioinformatic analysis of the *ScD27.2* promoter, a single conserved MYB motif (CAGTTG) was identified in the 371-bp fragment. Subsequently, we examined whether the drought-related transcription factor *ScMYB44* could bind to the *ScD27.2* promoter using a Y1H assay. The clones containing *ScMYB44* and the *ScD27.2* promoter demonstrated growth on SD/–Leu/AbA400 medium with the reporter strain, whereas the negative controls — containing either the pAbAi-pro*ScD27* vector alone or the empty pGADT7 AD vector — showed no growth (Fig. 10). These results demonstrate that ScMYB44 specifically binds to the *ScD27.2* promoter.

4. Discussion

Sugarcane, a C4 plant, demonstrates strong drought resistance and tolerance to barren conditions. Nevertheless, water and nutrient availability remain the primary factors limiting its vegetative growth. Research has established that strigolactones (SLs) function as important plant hormones in regulating abiotic stress responses (Umehara *et al.* 2010; Mayzlish-Gati *et al.* 2012; Foo *et al.* 2013; Cooper *et al.* 2018). The β-carotene isomerase D27 serves as the initial enzyme in the SL synthesis pathway, and the rice D27 gene encodes an iron-binding protein, β-carotene isomerase, which catalyzes the isomerization of all-*trans*-β-carotene in a reversible process (Wen *et al.* 2016; Wu *et al.* 2017; Shindo *et al.* 2018). *ScD27* possesses five homologues in *Saccharum spontanum* L. and belongs to the D27 clade endemic to land plants (Wu *et al.* 2017). The *ScD27.2* gene contains the DUF4033 domain, which potentially serves an important but non-essential biological function in enabling cellular adaptation to low nutrient conditions by inhibiting protein biosynthesis. These proteins bind to DUFs only when cells require nutrients, and most DUFs become necessary only under specific circumstances (Hauser *et al.* 2012). Analysis of the *ScD27.2* gene promoter activity and its regulatory elements suggests its involvement in the abiotic stress response in sugarcane. Subcellular localization revealed ScD27.2 in chloroplasts, consistent with the plastid localization of OsD27 and AtD27 (Lin *et al.* 2009; Waters

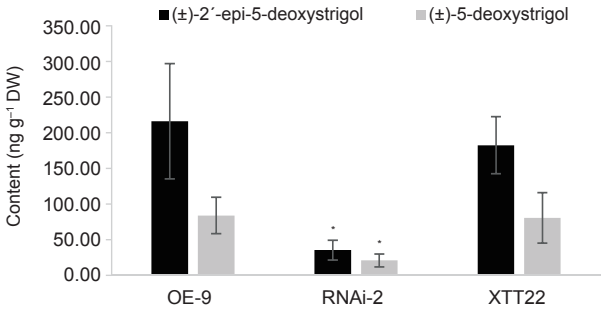


Fig. 9 Quantification of (±)-2′-epi-5-deoxystrigol and (±)-5-deoxystrigol in root tissues of wild-type sugarcane ('XTT22') and transgenic *ScD27*-OE-9 and *ScD27*-RNAi-2 specimens under drought conditions (*n*=6). Error bars indicate SE. Statistical significance relative to wild type control, calculated *via* Student's *t*-test assuming unequal variance, is denoted by asterisks for *ScD27*-RNAi-2 and *ScD27*-OE-9 compared to 'XTT22', where $P<0.05$ indicates significant difference.

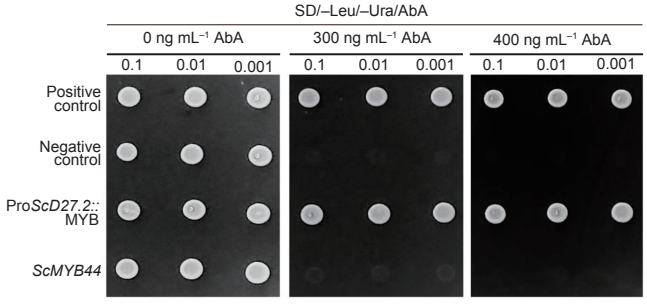


Fig. 10 Analysis of protein interactions between transcription factor *ScMYB44* and the *ScD27.2* promoter using yeast-one-hybrid (Y1H) assay. The *ScD27.2* promoter was positioned upstream of the Aureobasidin A resistance (*AbAr*) gene and incorporated into Y1HGold to generate the reporter strain. Following transformation with *ScMYB44* transcription factors, growth was monitored for 3 d at 30°C with and without 300 or 400 ng mL^{-1} AbA.

et al. 2012), further supporting the non-migration of the all-*trans* beta-carotene D27 precursor. The genomic sequence of *ScD27.2* comprised 7 exons and 6 introns, similar to the structure of the *D27* gene in most plants (Marzec and Muszynska 2015), indicating strong conservation of the *D27* genome sequence.

SL synthesis occurs primarily in the roots and potentially in the lower portions of the stalk (Dun *et al.* 2009; Lucido *et al.* 2022). Previous research has demonstrated high expression of *ScD27.2* in roots and significant expression in shoot tips (Wu *et al.* 2017). The present study revealed *ScD27.2* gene expression in various parts of sugarcane, with varying expression levels among plant tissues. The *ScD27.2* gene exhibited high expression in stalk tips and axillary buds, with peak expression observed in stem tips. Consequently, expression analysis in this study focused primarily on detecting *ScD27.2* expression in the shoot tip.

Using 'XTT22' sugarcane as recipient material, *ScD27.2* overexpression and silencing lines were constructed. Both overexpression and silencing of *ScD27.2* significantly affected sugarcane tillering. *ScD27*-OE-9 and *ScD27*-RNAi-2 exhibited marked differences in tillering phenotypes, demonstrating the regulatory role of *ScD27.2* gene in tillering (Delaux *et al.* 2012; Waters *et al.* 2012). The observed tiller phenotypes of *ScD27*-OE-9 and *ScD27*-RNAi-2 support the conserved function of *ScD27.2* (Delaux *et al.* 2012; Waters *et al.* 2012). Under normal watering conditions, *ScD27*-OE-9 produced significantly fewer tillers compared to 'XTT22', while maintaining similar plant height. The RNAi lines developed more tillers but exhibited significantly reduced height compared to the wild type. These findings suggest a negative correlation between the relative expression level of *ScD27.2* in sugarcane and tiller number.

The *ScD27.2* gene responds to various environmental stresses, including PEG stress, salt stress, phosphate deficiency, and nutrient deficiency (Wu *et al.* 2017). Previous research has examined D27 regulation in sugarcane under conditions of phosphate deficiency, dark treatment, and drought stress (Foo *et al.* 2005; Johnson *et al.* 2006; Crawford *et al.* 2010; Ward *et al.* 2013). Evidence suggests that *ScD27.2* functions as a critical abiotic stress response gene within the sugarcane SL biosynthesis pathway.

The present study demonstrates that *ScD27.2* significantly influences phosphate deficiency responses, light sensitivity, and drought stress tolerance in sugarcane. Notably, *ScD27.2* expression increased under phosphate-deficient conditions, aligning with observations of enhanced SL biosynthesis in lettuce and tomato (Ruiz-Lozano *et al.* 2016). Research indicates that genes involved in SL biosynthesis pathways may be upregulated during phosphate deficiency (Liu *et al.* 2011; Bonneau *et al.* 2013). Under phosphate-deficient conditions, both shoot and root phosphate content decreased markedly, accompanied by elevated SL levels (Wen *et al.* 2015). Phosphate depletion stimulates SL biosynthesis (Xi *et al.* 2015), with the SL pathway's response correlating to phosphate availability (Czarnecki *et al.* 2013). This suggests that the biological activity of SLs is correlated with phosphate deficiency, implying a potential mechanistic link.

In this study, *ScD27.2* expression increased rapidly without phosphate, consistent with findings in *Arabidopsis* (Mayzlish-Gati *et al.* 2012), *Medicago truncatula* (Bonneau *et al.* 2013), and chrysanthemum (Wen *et al.* 2016). While *ScD27.2* expression increased under phosphate deficiency in the wild type and overexpression lines, RNAi lines showed no change. Similar expression patterns have been documented for *CCD7*, *CCD8*, *MAX2*, and *D14*, with significant expression increases in buds under phosphate-free conditions, suggesting conserved and coordinated phosphate starvation signaling (Wen *et al.* 2015; Pan *et al.* 2016). Analysis of transcription factors and regulatory elements controlling SL biosynthesis gene expression revealed specific binding sites and regulatory mechanisms, elucidating how these genes respond to phosphate starvation signals.

Light conditions influence SL levels (Mayzlish-Gati *et al.* 2010), and SLs may function as downstream signals in responses to both low and high red:far-red (R:FR) ratios. (R:FR) ratios. Light also affects auxin sensitivity (Jia *et al.* 2014; Krishna and Finlayson 2014; Wang *et al.* 2022). Changes in light quality and intensity modify SL accumulation, suggesting their role in light stress regulation (Bharti *et al.* 2015; Wen *et al.* 2016; Thussagunpanit *et al.* 2017). Analysis

of the *ScD27.2* promoter revealed multiple light regulatory elements, indicating light signal influence on *ScD27.2* expression patterns. The research demonstrated that dark treatment suppressed *ScD27.2* expression. Dark conditions represent extreme shade, distinct from low/high R:FR ratios, potentially explaining the reduced *ScD27.2* expression under dark treatment. Light-induced *ScD27.2* expression appears related to multiple photoactive elements in its promoter region. The *ScD27.2* promoter contains various light-responsive elements that detect external light signals. These elements coordinate *ScD27.2* gene expression through interactions with transcription factors and regulatory proteins.

During extended drought stress, stomatal closure becomes essential to prevent water loss, leading to impaired photosynthesis and restricted vegetative growth in aboveground plant parts. This study demonstrated that prolonged drought treatment severely impacted sugarcane growth. The tiller numbers of 'XTT22' and overexpression lines decreased to an average of 1.33 per plant. The RNAi lines exhibited an average tiller number of 9.60, with reduced plant height. The findings indicated that *ScD27.2* exhibited a moderate regulatory effect on the tillering phenotype. This moderate effect might be attributed to the compensatory action of other homologous genes, consistent with the mild phenotype observed in the *D27* mutant in *Arabidopsis* compared to other biosynthetic gene mutants (Waters *et al.* 2012). Drought stress induced an increase in SL yield. Furthermore, the *ScD27.2* silenced line showed significantly reduced levels of (±)-2′-epi-5-deoxystrigol and (±)-5-deoxystrigol under drought stress. Based on the drought survival test results and water deficiency rate, evidence suggests that *ScD27.2* serves as a key regulator in sugarcane's drought stress response, including its influence on tiller number. To further validate the crucial regulatory role of *ScD27.2* in sugarcane's drought stress response and its impact on tillering, protein–protein interaction studies would be valuable in identifying proteins that interact with *ScD27.2* or its regulatory elements. Such investigations would illuminate the molecular mechanisms underlying *ScD27.2*'s function in drought stress response. Understanding these interactions could provide insights into how *ScD27.2* coordinates sugarcane's adaptation to drought conditions, potentially revealing novel targets for genetic modification to enhance drought tolerance and tillering capacity.

Drought conditions may enhance the expression of SL biosynthetic gene *ScD27.2* in stalks and roots (Shindo *et al.* 2018), leading to increased SL accumulation in roots and enhanced SL production in rice (Bruno and Al-Babili 2016). During sustained mild drought, SL production exhibits more pronounced increases (Haider *et al.* 2018). Similarly, tomatoes under drought stress show elevated SL levels, enhancing their drought stress response capability (Ruiz-Lozano *et al.* 2016). Plants employ various strategies to manage drought conditions. This study revealed that under long-term mild drought stress, sugarcane plants maintained survival and moderate growth while showing significantly increased accumulation of two SL types in the roots. These findings suggest these SLs serve a critical protective function in sugarcane's drought stress response. The observed effects of long-term mild drought stress on sugarcane, including growth inhibition, increased SL content, and reduced tillering, align with previous findings in rice (Zhang *et al.* 2010; Haider *et al.* 2018) and chrysanthemum (Dierck *et al.* 2016; Nie *et al.* 2018).

Xanthoceras sorbifolium XsMYB44 maintains water levels, reactive oxygen species (ROS) homeostasis, and plant response to drought and heat stress through stomatal closure regulation (Li *et al.* 2021). Research indicates that plant *MYB44* positively regulates plant response to abiotic stress by initiating stomatal closure to maintain water levels and regulate ROS homeostasis (Persak and Pitzschke 2014; Li *et al.* 2021). The present study demonstrated through Y1H assays that *MYB44* bound to the *ScD27.2* promoter, suggesting that *MYB44* may participate in the drought stress response of *ScD27.2*.

Sugarcane's highly polyploid nature and complex genetic background make gene discovery and functional identification more challenging compared to other crops (Zhang *et al.* 2018). The conserved characteristics among grass species suggest that sugarcane likely shares similar gene functions and regulatory networks with rice and maize. Although gene functions remain conserved, the resulting phenotypes and developmental impacts may be species-specific, with regulatory mechanisms potentially evolving differently across species. While the rice *D27* mutant exhibits a short stature (Lin *et al.* 2009; Umehara *et al.* 2010), our findings indicate that alterations in *ScD27.2* expression under normal conditions affected plant height, though not substantially. However, transgenic lines demonstrated significant height variations under prolonged drought conditions. Furthermore, the absence of significant changes in sugar content within *ScD27.2* transgenic lines indicates its potential application for improving sugarcane yield.

SL synthesis primarily occurs in roots and potentially in lower stalk regions (Dun *et al.* 2009). *ScD27.2* demonstrates high expression in roots and notable expression in shoot tips (Wu *et al.* 2017). Plant SL content remains extremely low and challenging to quantify (Lopez-Raez *et al.* 2008; Roumeliotis *et al.* 2012). SL biosynthesis appears subject to multiple control levels, with anabolic genes regulated through coordinated interactions between key plant hormones (Cheng *et al.* 2013; Marzec 2017; Omoarelojie *et al.* 2019). SLs promote abiotic stress recovery in *Arabidopsis* (Persak and Pitzschke 2014) and *Lotus japonicus* (Liu *et al.* 2015). SLs accumulate in plant tissues responding to suboptimal environmental conditions, including drought, salinity, temperature, nutrient deficiency, and oxidative stress (Kapulnik and Koltai 2014; Andreo-Jimenez *et al.* 2015; Pandey *et al.* 2016; Mostofa *et al.* 2018; Zhang *et al.* 2022). While their precise role remains unclear, SLs may trigger downstream osmotic enzyme expression to maintain metabolic homeostasis in stressed cells (Aroca *et al.* 2013; Raja *et al.* 2023; Tariq *et al.* 2023). Consequently, exogenous treatment or transgenic modification of SL bioaccumulation presents a potential strategy for enhancing crop and plant tolerance to multiple abiotic stressors (Saeed *et al.* 2017).

5. Conclusion

The *ScD27.2* gene represents a conserved component in the SL biosynthesis pathway that responds to abiotic stress and regulates sugarcane tillering, influenced by environmental factors such as drought, light, and phosphate stress. This study elucidates the mechanisms of sugarcane tillering under stress conditions and establishes a theoretical foundation for breeding high-yield sugarcane varieties. Future research will focus on different treatments, bud hormone levels, exogenous hormone treatment, and regulatory mechanisms.

Acknowledgements

This project was funded by the National Natural Science Foundation of China (31860405); the National Key Laboratory for Tropical Crop Breeding, China (NKLTCB-YAAS-2024-S05); the Yunnan Provincial Modern Agricultural Technology System, China; the Yunnan Provincial Science and Technology Innovation Talent Program, China (202305AD160041); the Yunnan Provincial "Xingdian Talent Support Program", China; the Yunnan Haizhi Station for Sugarcane Research Institute of Yunnan Academy of Agricultural Sciences, China (HHZ202201); and the Yunnan Provincial Key Research and Development Program, China (202403AM140025).

Declaration of competing interest

The authors declare that they have no conflict of interest.

Declaration of generative AI and AI-assisted technologies in the writing process

During the preparation of this work, the authors used DeepSeek in order to assist with language refinement and conceptual clarification. After using this tool, the authors reviewed and edited the content as needed and take full responsibility for the content of the published article.

Appendixces associated with this paper are available at https://doi.org/10.1016/j.jia.2025.04.017

References

de Abreu L G F, Grassi M C B, de Carvalho L M, Da Silva J J B, Oliveira J V C, Bressiani J A, Pereira G A G. 2020. Energy cane vs sugarcane: Watching the race in plant development. *Industrial Crops and Products*, **156**, 112868.

Abuauf H, Haider I, Jia K P, Ablazov A, Mi J, Blilou I, Al-Babili S. 2018. The Arabidopsis *DWARF27* gene encodes an all-*trans*-/9-*cis*-β-carotene isomerase and is induced by auxin, abscisic acid and phosphate deficiency. *Plant Science*, **277**, 33–42.

Aitken K S, Hermann S, Karno K, Bonnett G D, Mcintyre L C, Jackson P A. 2008. Genetic control of yield related stalk traits in sugarcane. *Theoretical and Applied Genetics*, **117**, 1191–1203.

Al-Babili S, Bouwmeester H J. 2015. Strigolactones, a novel carotenoid-derived plant hormone. *Annual Review of Plant Biology*, **66**, 161–186.

Alder A, Jamil M, Marzorati M, Bruno M, Vermathen M, Bigler P, Ghisla S, Bouwmeester H, Beyer P, Al-Babili S. 2012. The path from β-Carotene to carlactone, a strigolactone-like plant hormone. *Science*, **335**, 1348–1351.

Altschul S F, Madden T L, Schaffer A A, Zhang J, Zhang Z, Miller W, Lipman D J. 1997. Gapped BLAST and PSI-BLAST: A new generation of protein database search programs. *Nucleic Acids Research*, **25**, 3389–3402.

Andreo-Jimenez B, Ruyter-Spira C, Bouwmeester H J, Lopez-Raez J A. 2015. Ecological relevance of strigolactones in nutrient uptake and other abiotic stresses, and in plant–microbe interactions below-ground. *Plant and Soil*, **394**, 1–19.

Arite T, Iwata H, Ohshima K, Maekawa M, Nakajima M, Kojima M, Sakakibara H, Kyozuka J. 2007. DWARF10, an RMS1/MAX4/DAD1 ortholog, controls lateral bud outgrowth in rice. *Plant Journal*, **51**, 1019–1029.

Aroca R, Ruiz-Lozano J M, Zamarreño Á M, Paz J A, García-Mina J M, Pozo M J, López-Ráez J A. 2013. Arbuscular mycorrhizal symbiosis influences strigolactone production under salinity and alleviates salt stress in lettuce plants. *Journal of Plant Physiology*, **170**, 47–55.

Bari V K, Nassar J A, Aly R. 2021. CRISPR/Cas9 mediated mutagenesis of *MORE AXILLARY GROWTH 1* in tomato confers resistance to root parasitic weed *Phelipanche aegyptiaca*. *Scientific Reports*, **11**, 3905.

Batra R, Agarwal P, Tyagi S, Saini D K, Kumar V, Kumar A, Kumar S, Balyan H S, Pandey R, Gupta P K. 2019. A study of CCD8 genes/proteins in seven monocots and eight dicots. *PLoS ONE*, **14**, e0213531.

Bharti N, Tripathi S, Bhatla S C. 2015. Photomodulation of strigolactone biosynthesis and accumulation during sunflower seedling growth. *Plant Signaling & Behavior*, **10**, e1049792.

Bohorova N, Zhang W, Julstrom P, Mclean S, Luna B, Brito R M, Diaz L, Ramos M E, Estanol P, Pacheco M, Salgado M, Hoisington D. 1999. Production of transgenic tropical maize with *crylAb* and *crylAc* genes via microprojectile bombardment of immature embryos. *Theoretical and Applied Genetics*, **99**, 437–444.

Bonneau L, Huguet S, Wipf D, Pauly N, Truong H N. 2013. Combined phosphate and nitrogen limitation generates a nutrient stress transcriptome favorable for arbuscular mycorrhizal symbiosis in *Medicago truncatula*. *New Phytologist*, **199**, 188–202.

Brewer P B, Koltai H, Beveridge C A. 2013. Diverse roles of strigolactones in plant development. *Molecular Plant*, **6**, 18–28.

Bruno M, Al-Babili S. 2016. On the substrate specificity of the rice strigolactone biosynthesis enzyme DWARF27. *Planta*, **243**, 1429–1440.

Cao X, Liu Q, Rowland L J, Hammerschlag F A. 1998. GUS expression in blueberry (*Vaccinium* spp.): Factors influencing *Agrobacterium*-mediated gene transfer efficiency. *Plant Cell Reports*, **18**, 266–270.

Cheng X, Flokova K, Bouwmeester H, Ruyter-Spira C. 2017. The role of endogenous strigolactones and their interaction with ABA during the infection process of the parasitic weed *Phelipanche ramosa* in tomato plants. *Frontiers in Plant Science*, **8**, 392.

Cheng X, Ruyter-Spira C, Bouwmeester H. 2013. The interaction between strigolactones and other plant hormones in the regulation of plant development. *Frontiers in Plant Science*, **4**, 199.

Cooper J W, Hu Y, Beyyoudh L, Yildiz D H, Kunert K, Beveridge C A, Foyer C H. 2018. Strigolactones positively regulate chilling tolerance in pea and in Arabidopsis. *Plant Cell and Environment*, **41**, 1298–1310.

Crawford S, Shinohara N, Sieberer T, Williamson L, George G, Hepworth J, Muller D, Domagalska M A, Leyser O. 2010. Strigolactones enhance competition between shoot branches by dampening auxin transport. *Development*, **137**, 2905–2913.

Czarnecki O, Yang J, Wang X, Wang S, Muchero W, Tuskan G A, Chen J G. 2014. Characterization of *MORE AXILLARY GROWTH* genes in populus. *PLoS ONE*, **9**, e102757.

Czarnecki O, Yang J, Weston D J, Tuskan G A, Chen J G. 2013. A dual role of strigolactones in phosphate acquisition and utilization in plants. *International Journal of Molecular Sciences*, **14**, 7681–7701.

Delaux P M, Xie X, Timme R E, Puech-Pages V, Dunand C, Lecompte E, Delwiche C F, Yoneyama K, Becard G, Sejalon-Delmas N. 2012. Origin of strigolactones in the green lineage. *New Phytologist*, **195**, 857–871.

Dias H B, Sentelhas P C. 2018. Sugarcane yield gap analysis in Brazil — A multi-model approach for determining magnitudes and causes. *Science of the Total Environment*, **637–638**, 1127–1136.

Dierck R, De Keyser E, De Riek J, Dhooghe E, Van Huylenbroeck J, Prinsen E, Van Der Straeten D. 2016. Change in auxin and cytokinin levels coincides with altered expression of branching genes during axillary bud outgrowth in *Chrysanthemum*. *PLoS ONE*, **11**, e0161732.

Dun E A, Hanan J, Beveridge C A. 2009. Computational modeling and molecular physiology experiments reveal new insights into shoot

branching in pea. *Plant Cell*, **21**, 3459–3472.
Foo E, Bullier E, Goussot M, Foucher F, Rameau C, Beveridge C A. 2005. The branching gene *RAMOSUS1* mediates interactions among two novel signals and auxin in pea. *Plant Cell*, **17**, 464–474.
Foo E, Yoneyama K, Hugill C J, Quittenden L J, Reid J B. 2013. Strigolactones and the regulation of pea symbioses in response to nitrate and phosphate deficiency. *Molecular Plant*, **6**, 76–87.
Frey A, Effroy D, Lefebvre V, Seo M, Perreau F, Berger A, Sechet J, To A, North H M, Marion-Poll A. 2012. Epoxycarotenoid cleavage by NCED5 fine-tunes ABA accumulation and affects seed dormancy and drought tolerance with other NCED family members. *Plant Journal*, **70**, 501–512.
Gomez-Roldan V, Fermas S, Brewer P B, Puech-Pagès V, Dun E A, Pillot J, Letisse F, Matusova R, Danoun S, Portais J, Bouwmeester H, Bécard G, Beveridge C A, Rameau C, Rochange S F. 2008. Strigolactone inhibition of shoot branching. *Nature*, **455**, 189–194.
Ha C V, Leyva-Gonzalez M A, Osakabe Y, Tran U T, Nishiyama R, Watanabe Y, Tanaka M, Seki M, Yamaguchi S, Dong N V, Yamaguchi-Shinozaki K, Shinozaki K, Herrera-Estrella L, Tran L S. 2014. Positive regulatory role of strigolactone in plant responses to drought and salt stress. *Proceedings of the National Academy of Sciences of the United States of America*, **111**, 851–856.
Haider I, Andreo-Jimenez B, Bruno M, Bimbo A, Flokova K, Abuauf H, Ntui V O, Guo X, Charnikhova T, Al-Babili S, Bouwmeester H J, Ruyter-Spira C. 2018. The interaction of strigolactones with abscisic acid during the drought response in rice. *Journal of Experimental Botany*, **69**, 2403–2414.
Hauser R, Pech M, Kijek J, Yamamoto H, Titz B, Naeve F, Tovchigrechko A, Yamamoto K, Szaflarski W, Takeuchi N, Stellberger T, Diefenbacher M E, Nierhaus K H, Uetz P. 2012. RsfA (YbeB) proteins are conserved ribosomal silencing factors. *PLoS Genetics*, **8**, e1002815.
Hemaprabha G, Mohanraj K, Jackson P A, Lakshmanan P, Ali G S, Li A M, Huang D L, Ram B. 2022. Sugarcane genetic diversity and major germplasm collections. *Sugar Tech*, **24**, 279–297.
Hirayama T, Shinozaki K. 2007. Perception and transduction of abscisic acid signals: Keys to the function of the versatile plant hormone ABA. *Trends in Plant Science*, **12**, 343–351.
Iyer-Pascuzzi A S, Jackson T, Cui H, Petricka J J, Busch W, Tsukagoshi H, Benfey P N. 2011. Cell identity regulators link development and stress responses in the *Arabidopsis* root. *Developmental Cell*, **21**, 770–782.
Jia K P, Luo Q, He S B, Lu X D, Yang H Q. 2014. Strigolactone-regulated hypocotyl elongation is dependent on cryptochrome and phytochrome signaling pathways in *Arabidopsis*. *Molecular Plant*, **7**, 528–540.
Johnson X, Brcich T, Dun E A, Goussot M, Haurogne K, Beveridge C A, Rameau C. 2006. Branching genes are conserved across species. Genes controlling a novel signal in pea are coregulated by other long-distance signals. *Plant Physiology*, **142**, 1014–1026.
Kandel R, Yang X, Song J, Wang J. 2018. Potentials, challenges, and genetic and genomic resources for sugarcane biomass improvement. *Frontiers in Plant Science*, **9**, 151.
Kapulnik Y, Koltai H. 2014. Strigolactone involvement in root development, response to abiotic stress, and interactions with the biotic soil environment. *Plant Physiology*, **166**, 560–569.
Katoh K, Standley D M. 2013. MAFFT multiple sequence alignment software version 7: Improvements in performance and usability. *Molecular Biology and Evolution*, **30**, 772–780.
Koltai H, Cohen M, Chesin O, Mayzlish-Gati E, Bécard G, Puech V, Dor B B, Resnick N, Wininger S, Kapulnik Y. 2011. Light is a positive regulator of strigolactone levels in tomato roots. *Journal of Plant Physiology*, **168**, 1993–1996.
Krishna R S, Finlayson S A. 2014. Phytochrome B promotes branching in Arabidopsis by suppressing auxin signaling. *Plant Physiology*, **164**, 1542–1550.
Li J, Zhao S, Yu X, Du W, Li H, Sun Y, Sun H, Ruan C. 2021. Role of *Xanthoceras sorbifolium* MYB44 in tolerance to combined drought and heat stress via modulation of stomatal closure and ROS homeostasis. *Plant Physiology and Biochemistry*, **162**, 410–420.
Lin H, Wang R, Qian Q, Yan M, Meng X, Fu Z, Yan C, Jiang B, Su Z, Li J, Wang Y. 2009. DWARF27, an iron-containing protein required for the biosynthesis of strigolactones, regulates rice tiller bud outgrowth. *Plant Cell*, **21**, 1512–1525.
Liu J, He H, Vitali M, Visentin I, Charnikhova T, Haider I, Schubert A, Ruyter-Spira C, Bouwmeester H J, Lovisolo C, Cardinale F. 2015. Osmotic stress represses strigolactone biosynthesis in *Lotus japonicus* roots: Exploring the interaction between strigolactones and ABA under abiotic stress. *Planta*, **241**, 1435–1451.
Liu W, Kohlen W, Lillo A, Op D C R, Ivanov S, Hartog M, Limpens E, Jamil M, Smaczniak C, Kaufmann K, Yang W C, Hooiveld G J, Charnikhova T, Bouwmeester H J, Bisseling T, Geurts R. 2011. Strigolactone biosynthesis in *Medicago truncatula* and rice requires the symbiotic GRAS-type transcription factors NSP1 and NSP2. *Plant Cell*, **23**, 3853–3865.
Livak K J, Schmittgen T D. 2001. Analysis of relative gene expression data using real-time quantitative PCR and the $2^{-\Delta\Delta CT}$ method. *Methods*, **25**, 402–408.
Lofton J, Tubana B S, Kanke Y, Teboh J, Viator H, Dalen M. 2012. Estimating sugarcane yield potential using an in-season determination of normalized difference vegetative index. *Sensors*, **12**, 7529–7547.
Lopez-Raez J A, Charnikhova T, Gomez-Roldan V, Matusova R, Kohlen W, De Vos R, Verstappen F, Puech-Pages V, Becard G, Mulder P, Bouwmeester H. 2008. Tomato strigolactones are derived from carotenoids and their biosynthesis is promoted by phosphate starvation. *New Phytologist*, **178**, 863–874.
Lucido A, Basallo O, Sorribas A, Marin-Sanguino A, Vilaprinyo E, Alves R. 2022. A mathematical model for strigolactone biosynthesis in plants. *Frontiers in Plant Science*, **13**, 979162.
Mach J. 2015. Strigolactones regulate plant growth in arabidopsis via degradation of the DWARF53-like proteins SMXL6, 7, and 8. *Plant Cell*, **27**, 3022–3023.
Marzec M. 2017. Strigolactones and gibberellins: A new couple in the phytohormone world? *Trends in Plant Science*, **22**, 813–815.
Marzec M, Muszynska A. 2015. *In silico* analysis of the genes encoding proteins that are involved in the biosynthesis of the RMS/MAX/D pathway revealed new roles of strigolactones in plants. *International Journal of Molecular Sciences*, **16**, 6757–6782.
Mayzlish-Gati E, De-Cuyper C, Goormachtig S, Beeckman T, Vuylsteke M, Brewer P B, Beveridge C A, Yermiyahu U, Kaplan Y, Enzer Y, Wininger S, Resnick N, Cohen M, Kapulnik Y, Koltai H. 2012. Strigolactones are involved in root response to low phosphate conditions in Arabidopsis. *Plant Physiology*, **160**, 1329–1341.
Mayzlish-Gati E, Lekkala S P, Resnick N, Wininger S, Bhattacharya C, Lemcoff J H, Kapulnik Y, Koltai H. 2010. Strigolactones are positive regulators of light-harvesting genes in tomato. *Journal of Experimental Botany*, **61**, 3129–3136.
Meena M R, Appunu C, Arun K R, Manimekalai R, Vasantha S, Krishnappa G, Kumar R, Pandey S K, Hemaprabha G. 2022. Recent advances in sugarcane genomics, physiology, and phenomics for superior agronomic traits. *Frontiers in Genetics*, **13**, 854936.
Mostofa M G, Li W, Nguyen K H, Fujita M, Tran L P. 2018. Strigolactones in plant adaptation to abiotic stresses: An emerging avenue of plant research. *Plant Cell and Environment*, **41**, 2227–2243.
Murashige T, Skoog F. 1962. Revised medium for rapid growth and bioassays with tobacco tissue cultures. *Physiologia Plantarum*, **1**, 473–497.
Nie J, Wen C, Xi L, Lv S, Zhao Q, Kou Y, Ma N, Zhao L, Zhou X. 2018. The AP2/ERF transcription factor CmERF053 of chrysanthemum positively regulates shoot branching, lateral root, and drought tolerance. *Plant Cell Reports*, **37**, 1049–1060.
Omoarelojie L O, Kulkarni M G, Finnie J F, Van Staden J. 2019. Strigolactones and their crosstalk with other phytohormones. *Annals of Botany*, **124**, 749.
Pan X, Zheng H, Zhao J, Xu Y, Li X. 2016. ZmCCD7/ZpCCD7 encodes a carotenoid cleavage dioxygenase mediating shoot branching. *Planta*, **243**, 1407–1418.
Pandey A, Sharma M, Pandey G K. 2016. Emerging Roles of strigolactones in plant responses to stress and development. *Frontiers in Plant Science*, **7**, 434.
Pena J T, Sohn-Lee C, Rouhanifard S H, Ludwig J, Hafner M, Mihailovic A, Lim C, Holoch D, Berninger P, Zavolan M, Tuschl T. 2009. miRNA *in situ* hybridization in formaldehyde and EDC-fixed tissues. *Nature Methods*, **6**, 139–141.
Persak H, Pitzschke A. 2014. Dominant repression by Arabidopsis transcription factor MYB44 causes oxidative damage and hypersensitivity to abiotic stress. *International Journal of Molecular*

Sciences, **15**, 2517–2537.
Raja V, Qadir S U, Kumar N, Alsahli A A, Rinklebe J, Ahmad P. 2023. Melatonin and strigolactone mitigate chromium toxicity through modulation of ascorbate-glutathione pathway and gene expression in tomato. *Plant Physiology and Biochemistry*, **201**, 107872.
Rasmussen A, Depuydt S, Goormachtig S, Geelen D. 2013. Strigolactones fine-tune the root system. *Planta*, **238**, 615–626.
Roumeliotis E, Kloosterman B, Oortwijn M, Kohlen W, Bouwmeester H J, Visser R G, Bachem C W. 2012. The effects of auxin and strigolactones on tuber initiation and stolon architecture in potato. *Journal of Experimental Botany*, **63**, 4539–4547.
Ruiz-Lozano J M, Aroca R, Zamarreño Á M, Molina S, Andreo-Jiménez B, Porcel R, García-Mina J M, Ruyter-Spira C, López-Ráez J A. 2016. Arbuscular mycorrhizal symbiosis induces strigolactone biosynthesis under drought and improves drought tolerance in lettuce and tomato. *Plant*, *Cell & Environment*, **39**, 441–452.
Ruyter-Spira C, Al-Babili S, van der Krol S, Bouwmeester H. 2013. The biology of strigolactones. *Trends in Plant Science*, **18**, 72–83.
Saeed W, Naseem S, Ali Z. 2017. Strigolactones biosynthesis and their role in abiotic stress resilience in plants: A critical review. *Frontiers in Plant Science*, **8**, 1487.
Shindo M, Shimomura K, Yamaguchi S, Umehara M. 2018. Upregulation of *DWARF27* is associated with increased strigolactone levels under sulfur deficiency in rice. *Plant Direct*, **2**, e00050.
De Smet I, Signora L, Beeckman T, Inze D, Foyer C H, Zhang H. 2003. An abscisic acid-sensitive checkpoint in lateral root development of *Arabidopsis*. *Plant Journal*, **33**, 543–555.
Stirnberg P, Zhao S, Williamson L, Ward S, Leyser O. 2012. *FHY3* promotes shoot branching and stress tolerance in Arabidopsis in an *AXR1*-dependent manner. *Plant Journal*, **71**, 907–920.
Sun D, Guo T, Ran Y, Huang Y, Guan B O. 2014. *In-situ* DNA hybridization detection with a reflective microfiber grating biosensor. *Biosensors & Bioelectronics*, **61**, 541–546.
Tariq A, Ullah I, Sardans J, Graciano C, Mussarat S, Ullah A, Zeng F, Wang W, Al-Bakre D A, Ahmed Z, Ali S, Zhang Z, Yaseen A, Peñuelas J. 2023. Strigolactones can be a potential tool to fight environmental stresses in arid lands. *Environmental Research*, **229**, 115966.
Thussagunpanit J, Nagai Y, Nagae M, Mashiguchi K, Mitsuda N, Ohme-Takagi M, Nakano T, Nakamura H, Asami T. 2017. Involvement of STH7 in light-adapted development in *Arabidopsis thaliana* promoted by both strigolactone and karrikin. *Bioscience Biotechnology and Biochemistry*, **81**, 292–301.
Tolnai Z, Sharma H, Soos V. 2024. D27-like carotenoid isomerases: At the crossroads of strigolactone and abscisic acid biosynthesis. *Journal of Experimental Botany*, **75**, 1148–1158.
Umehara M, Hanada A, Magome H, Takeda-Kamiya N, Yamaguchi S. 2010. Contribution of strigolactones to the inhibition of tiller bud outgrowth under phosphate deficiency in rice. *Plant and Cell Physiology*, **51**, 1118–1126.
Umehara M, Hanada A, Yoshida S, Akiyama K, Arite T, Takeda-Kamiya N, Magome H, Kamiya Y, Shirasu K, Yoneyama K, Kyozuka J, Yamaguchi S. 2008. Inhibition of shoot branching by new terpenoid plant hormones. *Nature*, **455**, 195–200.
Wang T, Xu F, Wang Z, Wu Q, Cheng W, Que Y, Xu L. 2023. Mapping of QTLs and screening candidate genes associated with the ability of sugarcane tillering and ratooning. *International Journal of Molecular Sciences*, **24**, 2793.
Wang W, Gao H, Liang Y, Li J, Wang Y. 2022. Molecular basis underlying rice tiller angle: Current progress and future perspectives. *Molecular Plant*, **15**, 125–137.
Wang X, Niu Y, Zheng Y. 2021. Multiple functions of MYB transcription factors in abiotic stress responses. *International Journal of Molecular Sciences*, **22**, 6125.
Ward S P, Salmon J, Hanley S J, Karp A, Leyser O. 2013. Using Arabidopsis to study shoot branching in biomass willow. *Plant Physiology*, **162**, 800–811.
Waters M T, Brewer P B, Bussell J D, Smith S M, Beveridge C A. 2012. The Arabidopsis ortholog of rice DWARF27 acts upstream of MAX1 in the control of plant development by strigolactones. *Plant Physiology*, **159**, 1073–1085.
Wei C Q, Chien C W, Ai L F, Zhao J, Zhang Z, Li K H, Burlingame A L, Sun Y, Wang Z Y. 2016. The *Arabidopsis* B-box protein BZS1/BBX20 interacts with HY5 and mediates strigolactone regulation of photomorphogenesis. *Journal of Genetics and Genomics*, **43**, 555–563.
Wen C, Xi L, Gao B, Wang K, Lv S, Kou Y, Ma N, Zhao L. 2015. Roles of *DgD14* in regulation of shoot branching in chrysanthemum (*Dendranthema grandiflorum* 'Jinba'). *Plant Physiology and Biochemistry*, **96**, 241–253.
Wen C, Zhao Q, Nie J, Liu G, Shen L, Cheng C, Xi L, Ma N, Zhao L. 2016. Physiological controls of chrysanthemum *DgD27* gene expression in regulation of shoot branching. *Plant Cell Reports*, **35**, 1053–1070.
Wu Z D, Liu X L, Liu J Y, Zan F G, Li X J, Liu H B, Lin X Q, Chen X K, Su H S, Zhao P F, Wu C W. 2017. Cloning and expression analysis of key gene *ScD27* in strigolactones biosynthesis pathway. *Acta Agronomica Sinica*, **43**, 31–41. (in Chinese)
Xi L, Wen C, Fang S, Chen X, Nie J, Chu J, Yuan C, Yan C, Ma N, Zhao L. 2015. Impacts of strigolactone on shoot branching under phosphate starvation in chrysanthemum (*Dendranthema grandiflorum* cv. Jinba). *Frontiers in Plant Science*, **6**, 694.
Yang Y, Abuauf H, Song S, Wang J Y, Alagoz Y, Moreno J C, Mi J, Ablazov A, Jamil M, Ali S, Zheng X, Balakrishna A, Blilou I, Al-Babili S. 2023. The Arabidopsis D27-LIKE1 is a *cis/cis/trans*-β-carotene isomerase that contributes to Strigolactone biosynthesis and negatively impacts ABA level. *Plant Journal*, **113**, 986–1003.
Yoo S D, Cho Y H, Sheen J. 2007. Arabidopsis mesophyll protoplasts: A versatile cell system for transient gene expression analysis. *Nature Protocols*, **2**, 1565–1572.
Yuan C, Ahmad S, Cheng T, Wang J, Pan H, Zhao L, Zhang Q. 2018. Red to far-red light ratio modulates hormonal and genetic control of axillary bud outgrowth in chrysanthemum (*Dendranthema grandiflorum* 'Jinba'). *International Journal of Molecular Sciences*, **19**, 1590.
Zhang J, Zhang X, Tang H, Zhang Q, Hua X, Ma X, Zhu F, Jones T, Zhu X, Bowers J, Wai C M, Zheng C, Shi Y, Chen S, Xu X, Yue J, Nelson D R, Huang L, Li Z, Xu H, *et al.* 2018. Allele-defined genome of the autopolyploid sugarcane *Saccharum spontaneum* L. *Nature Genetics*, **50**, 1565–1573.
Zhang S, Li G, Fang J, Chen W, Jiang H, Zou J, Liu X, Zhao X, Li X, Chu C, Xie Q, Jiang X, Zhu L. 2010. The interactions among *DWARF10*, auxin and cytokinin underlie lateral bud outgrowth in rice. *Journal of Integrative Plant Biology*, **52**, 626–638.
Zhang X, Zhang L, Ma C, Su M, Wang J, Zheng S, Zhang T. 2022. Exogenous strigolactones alleviate the photosynthetic inhibition and oxidative damage of cucumber seedlings under salt stress. *Scientia Horticulturae*, **297**, 110962.
Zhou J, Ma L, Zhang S, Zhu Y, Sun D. 2001. Extracellular calmodulin stimulates light-independent RbcS-GUS expression in suspension-cultured cells of transgenic tobacco. *Plant and Cell Physiology*, **42**, 1049–1055.
Zou J, Zhang S, Zhang W, Li G, Chen Z, Zhai W, Zhao X, Pan X, Xie Q, Zhu L. 2006. The rice *HIGH-TILLERING DWARF1* encoding an ortholog of Arabidopsis MAX3 is required for negative regulation of the outgrowth of axillary buds. *Plant Journal*, **48**, 687–698.

Executive Editor-in-Chief Sanwen Huang
Managing Editor Lingyun Weng